Developments in the Built Environment 17 (2024) 100370

Contents lists available at ScienceDirect

Developments in the Built Environment

journal homepage: www.sciencedirect.com/journal/developments-in-the-built-environment

A technical-environmental comparison of hybrid and blended slag cement-based recycled aggregate concrete tailored for optimal field performance

Juan Manuel Etcheverry [a,*], Agustin Laveglia [a,b], Yury Andres Villagran-Zaccardi [a,c], Nele De Belie [a,**]

[a] Magnel-Vandepitte Laboratory for Structural Engineering and Building Materials, Ghent University, Technologiepark-Zwijnaarde 60, 9052, Ghent, Belgium
[b] Institute of Construction and Building Materials, Faculty of Civil and Environmental Engineering,TU Darmstadt, Franziska-Braun-Straße 3, 64287, Darmstadt, Germany
[c] Sustainable Materials, Flemish Institute for Technological Research (VITO), Boeretang 200, 2400, Mol, Belgium

A B S T R A C T

The eco-design of concrete, employing a hybrid binder (HB) and recycled aggregates (RA), stands as a potential alternative for reducing CO_2 emissions. This research assesses the impact of three RA percentages and HB/commercial CEM III/B binders on concrete formulations in terms of technical performance (compressive strength (CS), carbonation (D_C), chloride migration (D_{Cl}), and transport properties. Results indicate that RA percentage is a more critical variable than the type of binder. Life-cycle assessment from cradle-to-gate reveals comparable CO_2 emissions for all concrete formulations. Incorporating concrete design parameters such as CS, D_C, and D_{Cl} in the functional unit shows carbon reductions between 10 and 60% for HB, with a diminishing benefit as the %RA increases. This underscores the potential of eco-designed concrete, particularly with HB, in achieving significant carbon footprint reductions. Careful consideration of RA percentages is essential for optimizing environmental benefits.

1. Introduction

Previous studies at the paste and mortar scale proved the suitability of increasing the compressive strength of binders containing a high amount of ground granulated blast furnace slag GGBFS by adding sodium sulfate (Rashad, 2015)– (Rashad et al., 2012). The alkaline activator interacts with the binder mainly at early ages controlling the fresh state properties (Etcheverry et al., 2023a). This is an advantage for practical applications because the w/b ratio can be fixed (based on durability requirements) and the strength of the concrete can be tailored (without modifying the kg of binder per m^3 of concrete) by changing the dosage of the activators (Etcheverry et al., 2023a), by engineering the slag fineness (Rashad et al., 2013) or even changing the amount of cement (Rashad, 2015). It is important to understand that the activator not only interacts with the cement but also with the GGBFS, increasing its reaction degree at early ages, accelerating the formation of C(-A)-S-H (calcium aluminosilicate hydrates), and forming more ettringite and AFm (aluminate ferrite monosubstituted) phases (Etcheverry et al., 2023a). The faster microstructure development raises the compressive strength as a results of a denser pore structure (Etcheverry et al., 2023b). Overall, and regardless the mechanisms taking place, the addition of activator has shown benefits for early age strength at paste and mortar scale. The reason behind choosing sodium sulfate as an activator for the hybrid systems is the reduced carbon-footprint in comparison to other alternatives, its availability as industrial by-product and the good performance in presence of Portland cement (Fu et al. 2020), (Acevedo--Martinez et al., 2012), (Mota et al., 2015).

In the literature, the use of hybrid systems is receiving more attention, but studies evaluating technological properties at concrete scale are still limited (Fu et al., 2021a), (Fu et al., 2021b)– (Joseph et al., 2019). This is essential for industrial application. Also, since the alkaline activator plays a fundamental role in strength gain, some differences could be expected when moving from paste or mortar scale to concrete, where the binder is only a fraction in volumetric terms. The use of recycled aggregates (RAs) is becoming more and more accepted in Europe due to the need to move towards a circular economy. Quarries are located farther and farther from urban centres, and transport distances are increasingly influencing the price and emissions associated with the product (European Environment Agency, 2008). Waste concrete is widely available in large urban centres but in many countries

* Corresponding author.
** Corresponding author.
E-mail addresses: juanmanuel.etcheverry@ugent.be (J.M. Etcheverry), Nele.DeBelie@ugent.be (N. De Belie).

https://doi.org/10.1016/j.dibe.2024.100370
Received 22 November 2023; Received in revised form 29 January 2024; Accepted 13 February 2024
Available online 17 February 2024

still mostly used for subflooring (downcycling) (Marsh et al., 2022) whereas its applications for structural concrete is still limited to low percentages: 20% in Annex 15 of the EHE-08, 30% for reinforced concrete in EI (dry indoor environment) or EE1 (humid indoor/outdoor environment 1), 20% for reinforced concrete in EE2, EE3, or EA1 (chemical aggressive environment 1), or 0% for more aggressive environments in NBN B15-001 (and up to 50% coarse RA class A+ for non-reinforced concrete in exposure class X_o -"no risk of corrosion or attack" for EN 206-1). Secondary resources represent a valuable source of raw materials to be used as RAs. Certainly, the inclusion of RA has an important impact on the quality of the resulting recycled aggregate concrete (RAC). The durability of RAC has been extensively studied and there is no consensus in the literature on the subject (Mcneil and Kang, 2013), (Villagrá et al., 2022). This is due to the great variability in the quality of the RA, as well as in the design of the mixes (Di Maio, 2010).

In this study, the performance of RA concrete made with a hybrid slag binder is evaluated. Concretes with a low initial carbon footprint can be produced by employing these two strategies together. To ensure that such concrete is more eco-efficient than its commercial equivalent, it is necessary to evaluate its behaviour in different scenarios. Previous studies highlighted not only the suitability of hybrid binder but also the necessity of upscaling the work done at paste and mortar level to concrete (Joseph et al., 2019), (Bernal, 2016), (Xue et al., 2021). Thus, the objective of this paper is to observe the microstructure development and evaluate the transport properties of these concretes produced with different percentages of RAs and compare them to equivalents with a commercial CEM III/B binder. The optimization of the granular skeleton by packing techniques such as Fuller or Bolomey curves can significantly reduce the carbon footprint of concrete (Scrivener et al., 2018). More complex techniques such as the Equivalent Mortar Replacement method and Direct Volume Replacement can be even more effective (Abbas et al., 2009). However, these tend to produce dry concrete with little slump. In the present work we opted for the design of somewhat more fluid concrete – class S3/S4 (BS EN 12350-2) without superplasticizers due to the limited information on the interaction between hybrid systems and commercial superplasticizers.

A secondary, but not less important objective is to assess the influence of the RA on the durability and transport properties of the concrete, as well as the influence of the binder type. The role of each variable in terms of the environmental impact is quantified through life-cycle assessment methodology. The most efficient solution in terms of global warming potential is discussed, taken into consideration the desired properties in the field.

2. Material and methods

2.1. Material characterization and mix design

The binders used in this study were a market available CEM III/B 42,5 N, Portland cement (PC) CEM I N 52,5 and ground granulated blast furnace slag (GGBFS). The chemical composition and physical characteristics of the binders are summarized in Table 1. The activator for the hybrid system was sodium sulfate, which was added as a dry powder (technical grade 99% purity) into the mix. Round shaped river gravel with sizes 2–8 mm, 8–16 mm and siliceous sand (0–4 mm) were used as natural aggregates. An RA from construction and demolition waste (C&DW) 1–16 mm partially replaced the natural aggregates in 4 out of 6 mixes. This industrially produced RA comprised >90% of crushed concrete, mortar, and unbound natural aggregate. The gradation and physical characteristics of each of the aggregates are shown in Fig. 1 and Table S1 (supporting information file).

The granular skeleton for the six concrete mixes was adjusted following the Fuller curve to optimise the particle size distribution. It minimizes the content of voids in the skeleton and the demand of paste in the concrete mix. The absorption of the natural aggregates (<0.5% in all cases) was corrected by adding an amount of mixing water

Table 1
Chemical composition determined by X-ray fluorescence analysis, and physical properties of the cements and GGBFS used.

Chemical composition [% m/m]	CEM III/B	PC (CEM I)	GGBFS
CaO	46.60	64.30	40.80
SiO_2	29.10	18.30	33.30
MgO	5.90	1.40	7.84
Al_2O_3	10.30	5.20	12.30
Fe_2O_3	1.50	4.00	0.39
Mn_2O_3	–	–	0.36
Cl	0.04	0.06	–
BaO	–	–	0.31
SO_3	2.70	3.50	2.30
Na_2O	0.90	0.32	0.44
K_2O	–	0.43	0.67
TiO_2	–	–	2.30
Insoluble residue	1.30	0.40	–
CaO + MgO + SiO_2	81.61	84.00	81.94
(CaO + MgO)/SiO_2	1.80	3.59	1.46
Physical Properties			
Particle size distribution (μm) d10/ d50/d90	2.8/10.0/ 27.4	2.3/10.8/ 29.4	1.3/7.6/ 26.8
Density[a] [kg/m^3]	2980	3160	2890

[a] Determined according to EN 196-6.

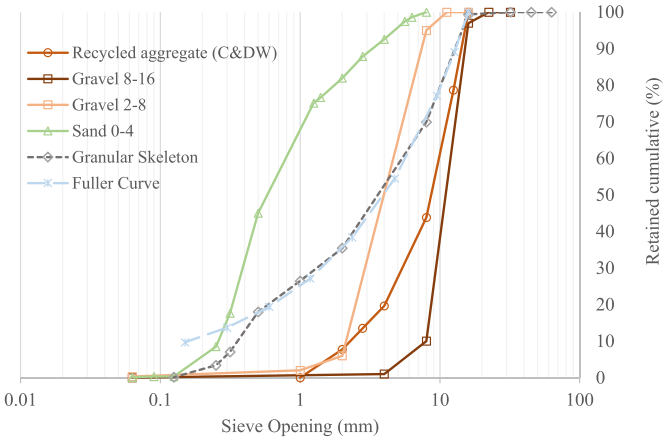

Fig. 1. Gradation of aggregates and resulting granular skeleton produced with natural and recycled aggregates.

corresponding to 100% of their water absorption, while for the RA (8.3% water absorption for the 5–16 mm fraction and 14.6% for the 1–5 mm fraction) the total volume of mixing water was corrected by adding 65% percent of their water absorption. This value was determined experimentally by preparing smaller batches of concretes aiming at a S4 slump class (15–21 cm) and a compressive strength of 30 MPa at 7 days. Corrections between 65 and 70% of the water absorption are also found in the literature for low-quality coarse RA (Joa, 2013). The amount of paste was slightly increased in RAC mixes in order to mitigate differences in slump caused by the shape and roughness between the natural and the recycled aggregates (Table 2). Superplasticizers were not used to produce the concrete because of the unknown interaction with the hybrid binder. Table 2 shows the mix design for six concretes containing different percentages of RA, three of them produced with an experimental hybrid binder and three with a market-available CEM III/B.

For the production of concrete, the aggregates and their absorption water were mixed for 2 min, then the binder and the remaining water were added and mixed for 3 more minutes. The slump and temperature of the concrete were measured. Additionally, the unit weight and the air content of the mixes were measured according to EN 12350 (parts 2, 6 and 7). Later, the all the moulds were filled and compacted in 2 layers by means of a vibrator. The moulds were placed in a wet room (>95% RH and 20 °C). After one day, the specimens were demoulded and kept in

Table 2
Mix design for concrete produced with a hybrid and a blended binder and a variable RA content.

Materials (kg/m^3)	SS8 0RA	SS8 20RA	SS8 50RA	CEM III/B 0RA	CEM III/B 20RA	CEM III/B 50RA
Water	170	186	212	170	186	212
PC	102	102	104	–	–	–
GGBFS	238	240	243	–	–	–
CEM III/B	–	–	–	341	343	347
Na_2SO_4	19	19	19	–	–	–
Siliceous sand 0–4 mm	736	728	722	736	728	722
Gravel 2–8 mm	552	437	270	552	437	270
Gravel 8–16 mm	552	437	270	552	437	270
RA 1–16 mm	–	218	541	–	218	541
Effective w/b ratio	0.45	0.45	0.45	0.45	0.45	0.45

the wet room up to testing times of 28 and 90 days. Fig. 2 shows the part of each specimen used for the different experiments in this study. At least three samples were tested for each test in this study.

2.2. Ultrasonic pulse velocity measurements

The FreshCon device (University of Stuttgart) (Reinhardt and Grosse, 2004) continuously measured the evolution of the ultrasonic pulse velocity (UPV) in the concrete mixtures during setting and hardening. The device was located in a controlled environment (20 °C and 60% relative humidity). The dedicated FreshCon moulds (European Environment Agency, 2008) were filled and compacted in two layers. Immediately after, moulds were covered with polypropylene film to avoid excessive water evaporation. The ultrasonic pulse velocity, including longitudinal (P) and shear (S) waves, was recorded for 24 h. Data were obtained using the SmartPick software. The onset time of P-wave was selected based on the Akaike information criterion (AIC) (Reinhardt and Grosse, 2004) adapted to ultrasonic signals by (Krü et al., 2016). The onset time of the S-wave was determined by the transformation of the time signal into a time-frequency domain by means of a continuous wavelet transformation. Further details about mould dimensions, software and the P-wave and S-wave onset time pickers and FreshCon device are found in (Kurz et al., 2005)– (Smartmote - Universit ä and t Stuttgart, 2012). UPV setting times (P-wave curves) were determined based on the inflection point of the curve (Trtnik and Gams, 2013).

2.3. Compressive strength

Compressive strength (CS) tests were performed on cubes of 150 × 150 × 150 mm^3 according to the standard EN 12390–3:2019. Three concrete cubes per mix were tested at 1, 3, 7, 28, and 90 days of hydration.

2.4. Water absorption, capillary imbibition rate and density

After 28 and 90 days of curing, the specimens were submerged in water for 72 h (with all the surfaces exposed). The saturated-surface-dry and submerged weights were recorded. Samples were then dried at 40 °C and weighed daily until the weight difference between 2 successive measurements was smaller than 0.1%. Samples were placed into a plastic bag and kept in a climatized room at 20 °C and 65% RH for one more day. Capillary imbibition experiments were performed according to (IRAM, 1871:2021), with the only difference that samples were oven-dried at 40 °C instead of the 50 °C specified in the standard. The weight gain was recorded at 15, 30, 45, 60, 90, 120, 180, 240, 300 and 360 min within the first test day, and then every 24 h until the weight difference between consecutive measurements was smaller than 0.5%.

2.5. Rapid chloride migration test (CMT)

After 28 and 90 days in a wet room the specimens were dried at 40 °C until the weight difference between 2 successive measurements (24 ± 1 h) was smaller than 0.5%. Samples were placed in plastic bags and kept in a 20 °C and 65% RH room for one more day. Samples were moved to a desiccator, and vacuum was applied for 2 h. With vacuum still in place, samples were then impregnated with a saturated $Ca(OH)_2$ solution, vacuum was released and samples remained in immersion for a total of 24 h. Then, specimens were placed in a migration cell, with a catholyte solution (10% NaCl) at one side and an anolyte solution (0.3 N NaOH) at the other. The CMT test was performed as described in NT BUILD 492:1999 (Nordtest method).

2.6. Resistivity

The resistivity was measured before placing the saturated samples in the container for the rapid CMT. The resistivity was also recorded in samples impregnated with water, following a similar procedure as for CTM but using demineralized water instead of the $Ca(OH)_2$ solution. The resistivity was measured in the concrete discs with the direct method, by interposing the sample between the two plates with electrical contact

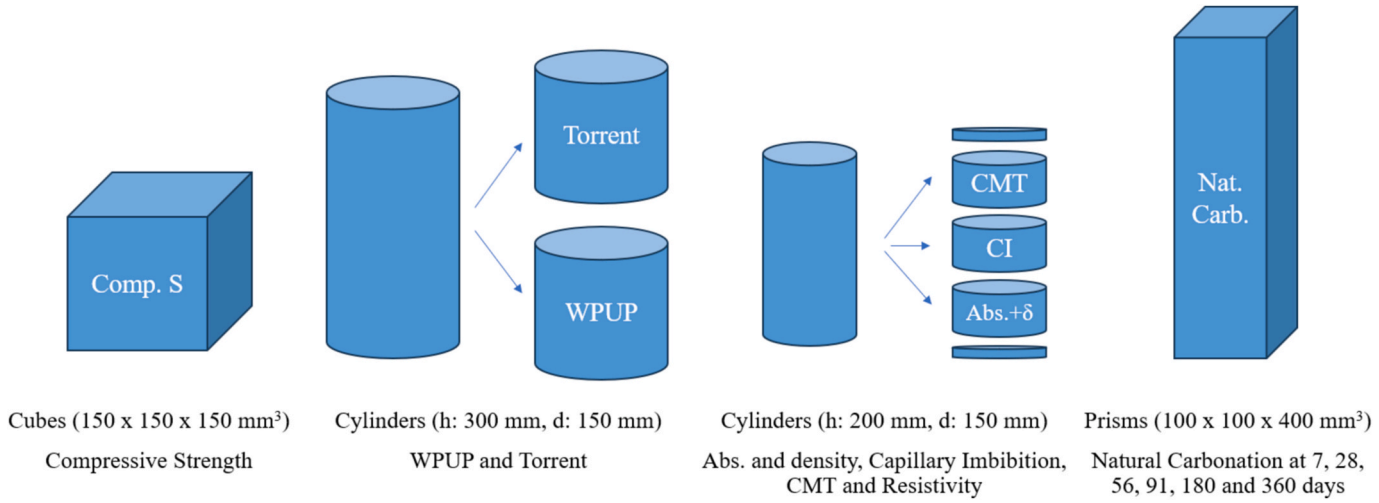

Fig. 2. Schematic representation of samples used for different experiments. WPUP stands for water penetration under pressure, Abs. for absorption and CMT for chloride migration test.

aided by moistened mats, and applying and electrical field across the sample while registering the ratio between voltage and current. The resistance of the mats was recorded beforehand and these values were subtracted from the final resistance values.

2.7. Water penetration under pressure and Torrent measurements

Concrete cylinders of 150 mm diameter and 300 mm height were sawn in two halves and the sawn face of the lower part (150 mm diameter and 150 mm height) was used to test water penetration under pressure (Fig. 2). After curing times of 28 and 90 days, specimens were preconditioned in a room at 20 °C and 65 % RH until the saturation degree of the sample was below 70%. Immediately after, three specimens per mix were placed in the testing device, with the sawn surface facing downwards and exposed to water penetration. Rubber rings were placed in between the specimens and the testing device to obtain a testing area of 100 mm diameter centred at the moulding face. The setup was tightened tightly in order to avoid water leakage or losses in the pressure. The cylinders were tested according to NBN EN 12390-8, for which 1 bar of water pressure was applied during the first 24 h and then increased up to 5 bar for two more days. Once the test was finished, the cylinders were removed from the permeameter, split in two halves and the penetration profile was recorded.

The remaining top parts (150 mm diameter and 150 mm height) obtained from the 150 mm diameter and 300 mm height concrete cylinders (Fig. 2) were cured and preconditioned in a room at 20 °C and 65 % RH until the humidity of the sample was below 70%. Immediately after, the sawn surface of three specimens per mix were tested and the KT value was determined using the Torrent permeameter according to SIA 262/1 Annex E.

2.8. Natural carbonation measurements

For each concrete mix, three 100 × 100 × 400 mm^3 concrete prisms were cast for carbonation evaluation. The specimens were demoulded 1 day later and kept for 27 more days in a room at >95% RH and 20 °C. The specimens were wrapped with plastic film and preconditioned in a room at 65% RH and 20 °C for 28 more days. Immediately after, samples were unwrapped, exposed to natural carbonation (in a controlled environment indoor, at 65% RH and 20 °C). One 70 mm-thick piece was split from each of the specimens after 7, 28, 56. 91, 180, and 360 days of exposure for the determination of the carbonation depth. The carbonation front was determined by spraying the freshly exposed surface with phenolphthalein at 1% solution in 70% Ethanol. The reported values are the average of three measurements per side (4) per specimen (3). The carbonation coefficient was obtained as a linear regression (with the square root of time) of the carbonation depth measured between 7 and 360 days of exposure.

2.9. Life-cycle assessment calculations

The Life-cycle Assessment (LCA) methodology (ISO 14040/44, 2006) is used to calculate the environmental impact over the life-cycle of the each studied concrete. Four main steps are performed: 1) definition of goal and scope, 2) inventory analysis, 3) life-cycle impact analysis and 4) interpretation of results (Laveglia et al., 2023), (Laveglia et al., 2022).

2.9.1. Goal and scope definition

This study aims at quantifying the enhanced sustainability of concrete mixes involving two circular economy strategies (CES) in comparison to the reference concrete CEM III/B 0RA (Table 2). The first strategy is comprehending the use of RA as replacement of 20 or 50% of the natural aggregates (CEM III/B 20RA and CEM III/B 50RA, respectively). The second strategy involves the use of a hybrid alkali activated binder with GGBFS, PC and RA (SS8 0RA, SS8 20RA, SS8 50RA). The system boundaries of the study are shown in Fig. 3. As a first approach, the $CO_{2\ C}$ indicator is calculated, standing for the kg of CO_2 emitted per cubic meter of concrete produced from cradle-to-gate of the factory, involving all required intermediate treatments for the conditioning of the C&DW and the GGBFS.

The cradle-to-gate boundaries are expanded to the use-phase by considering the mechanical and durability properties of each concrete. To account for the mechanical performance of each concrete formulation, the $CO_{2\ C}$ indicator is divided by the experimental compressive strength at a specific curing age (CSt), resulting in the $CO_{2\ CS}$ indicator, which expresses the CO_2 emissions per m^3 of concrete to deliver 1 MPa of strength (Eq. (1)). A major concern in reinforced concrete structures is the steel corrosion caused by the diffusivity of chlorides (D_{cl}) and carbonation (D_{CO2}) (See section 2.5 and 2.8 respectively). To compare the CES concretes against the reference, a modified approach was applied, as proposed by (Xue et al., 2021) based on the calculation of $CO_{2\ DI}$ and $CO_{2\ DII}$ indicators where the durability properties are integrated in $CO_{2\ CS}$. This approach, shown in Eqs. (2)–(4), considers a correction factor for the CO_2 emissions while keeping a comparable technical performance, based on the diffusion coefficients of the novel concrete in comparison to the reference. The chloride and carbonation resistance are accounted for in Eqs. (2) and (3), respectively, while the combined effect of chloride diffusion and carbonation is integrated in Eq. (4). In these equations i represent the specific CES and R the reference concrete formulation (CEM III/B 0RA). In all cases the properties determined at 90 days were used for the calculations.

$$CO_{2CS} = \left(\frac{CO_{2\ Ci}}{CS_t}\right) \quad \text{Equation 1}$$

$$CO_{2DI} = \left(\frac{CO_{2\ CS_i}}{CO_{2\ CS_R}}\right) * \left(\frac{D_{Cl_i}}{D_{Cl_R}}\right) \quad \text{Equation 2}$$

$$CO_{2DII} = \left(\frac{CO_{2\ CS_i}}{CO_{2\ CS_R}}\right) * \left(\frac{D_{CO_{2i}}}{D_{CO_{2R}}}\right) \quad \text{Equation 3}$$

$$CO_{2DC} = \left(\frac{CO_{2\ CS_i}}{CO_{2\ CS_R}}\right) * \left(\frac{D_{Cl_i}}{D_{Cl_R}}\right) * \left(\frac{D_{CO_{2i}}}{D_{CO_{2R}}}\right) \quad \text{Equation 4}$$

2.9.2. Life-cycle inventory and impact assessment

The life-cycle inventory (LCI) relates to the life-cycle phases accounted for during the impact calculation. In the case of the cradle-to-gate of the factory stage, the life-cycle inventories for the intermediate treatments required to produce RA and GGBFS were calculated following a process-based methodology according to a previous work of the authors (Laveglia et al., 2023). The following considerations were made.

- For the regionalization of the impacts, the current electricity and fuel mixes in Belgium based on a previous work by the authors have been applied (Laveglia et al., 2022).
- The C&DW used as RA is considered as a waste with no allocation of environmental impacts to its generation. The C&DW is transported to an integrated recycling plant at a distance of 100 km. At the plant, the material goes through a primary crushing operation, a classifying operation, and a secondary crushing. No allocation is attributed to each fraction.
- The blast furnace slag is a by-product of the steel production, and the intermediate treatment to produce the GGBFS includes granulation, drying and grinding operations. An economic allocation procedure based on a previous work is applied (Etcheverry et al., 2023a), in which 0.84% of the impacts related to the steelmaking process are allocated to the GGBFS production.

The cradle-to-gate LCI is shown in Table A1-A5 in the supporting information file. Ecoinvent Database V 3.6 is used to model the

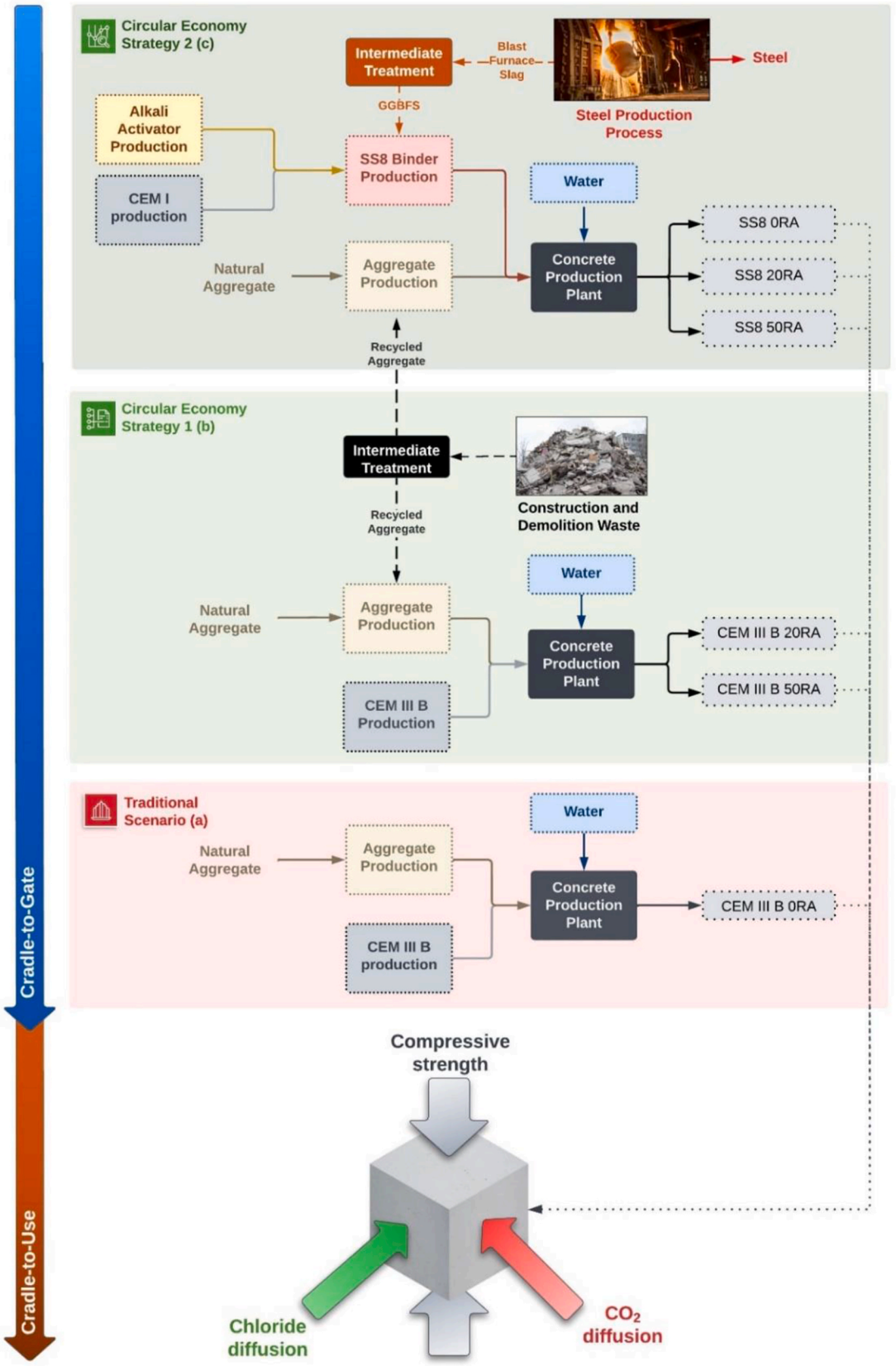

Fig. 3. System boundaries considered in the study. The traditional manufacturing scenario of concrete (a) is compared against two circular economy strategies: (b) use of C&DW as RA and (c) use of C&DW as RA in combination with an alkali activated hybrid binder. The use phase considers the mechanical and durability properties of the concrete mixes.

production systems. To account for the performance in the use phase, the experimental results of the compressive strength, chloride diffusion coefficient, and carbonation coefficient of the concrete mixes are considered.

The software OpenLCA is used to run the calculations. The CO_2 emissions associated to the manufacturing of each concrete are calculated using the impact method Impact 2002+b (Jolliet et al., 2003).

3. Results and discussion

3.1. Fresh state properties

Table 3 shows the fresh properties of the concrete mixes produced with the hybrid binder and the CEM III/B and variable contents of coarse RA from 0 to 50%. There seems to be a higher influence of the binder type than of the RA content on the slump. This confirms that the additional water to compensate for the absorption of the RA was correctly estimated. The addition of the activator increases the temperature of the concrete slightly. Even with the activator addition, better workability values were obtained for the hybrid binder than for the commercial cement CEM III/B. Since the CEM III/B is not necessarily finer than the hybrid binder (Table 1), there seems to be an effect of the sodium sulfate addition. To confirm this behaviour, five mortar mixes containing variable amount of sodium sulfate (0–10% wt. GGBFS) and 30% PC and 70% GGBFS were prepared and the flow was measured according to EN 1015-3. For more details about the mixes the reader is referred to (Etcheverry et al., 2023a). The results are plotted in Fig. 4, which confirms that the addition of the activator increases the workability at mortar and concrete scale.

Increasing the amount of RA in the concrete results in a reduction of the fresh density (unit weight in ASTM standards). This is consistent with the lower density of the recycled aggregates in comparison to the natural ones (Table 1). When it comes to the air content of the mixes, the differences are limited. There is a trend that the amount of RA seems to increase the air content of the hybrid concrete mixes, while a similar air content is observed for concrete made with a CEM III/B.

3.2. Setting and hardening process

Fig. 5 shows the development of microstructure of concrete mixes (hybrid binder) produced with variable amounts of RA measured by ultrasonic pulse velocity. The setting time calculated from P-wave curves (inflexion point of the cumulative curve or maximum of the derivative one) is indicated with vertical dotted lines in Fig. 5. UPV setting times are comparable among concrete mixes despite the amount of RA is increased from 0% to 20% and 50%. All UPV setting times were found to be in the range 230–260 min. Nevertheless, UPV measurements show that as hydration goes on, the RA take part of that free water. This is why the use of 50% RA shows a greater ultrasonic pulse velocity (S-waves) after 700 min when compared to 20%RA. The values are in very good agreement with the compressive strength reported at one day in next section. When it comes to the influence of RA in the development of microstructure for mixes containing CEM III/B, a similar ultrasonic pulse velocity is observed due to the limited hydration of CEM III/B during the first day (Fig. S1 supporting information file).

Table 3
Fresh state properties of concrete mixes produced with a hybrid and a blended binder and a variable RA content.

Designation	Slump (cm)	Temp.(°C)	Fresh density (kg/m^3)	Air content (%)
SS8 0RA	17	23	2350	1.7
SS8 20RA	18	19	2325	2.0
SS8 50RA	17	23	2250	2.6
CEM III/B 0RA	14	18	2331	2.3
CEM III/B 20RA	15	18	2294	2.3
CEM III/B 50RA	13	18	2244	2.3

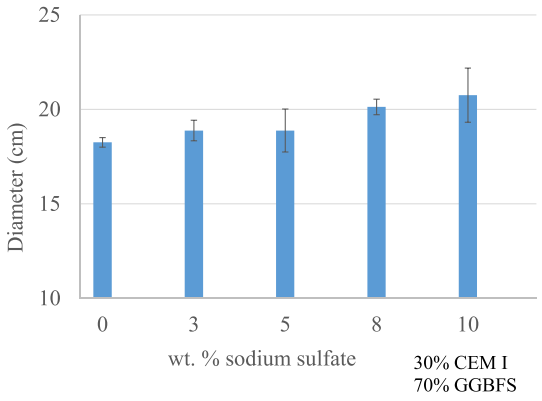

Fig. 4. Flow table measurements in mortars containing 30% PC, 70% GGBFS and sodium sulfate from 0 to 10 wt% respective to GGBFS).

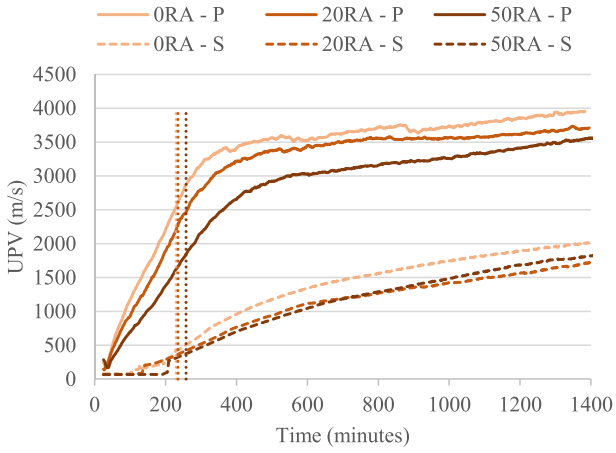

Fig. 5. FreshCon measurements on concrete mixes containing 0%, 20% and 50% RA and a hybrid binder. P-wave curves are plotted in full lines and S-wave curves in dashed lines. Vertical dotted lines indicate the initial setting times calculated from P-wave curves.

3.3. Strength development

Fig. 6 shows the values of compressive strength at 1, 3, 7, 28, and 90 days of hydration. At one day, the performance of the hybrid binder exceeds the one of the commercial cement regardless the amount of RA. Taking CEM III/B series as a reference, the hybrid system provides a compressive strength at one day that is 4 times higher for concrete without RA and 2–3 times higher for concrete with 20–50% RA. At 3 days of hydration, the use of the hybrid binder still results in a 25%–75% higher strength. This is the result of sodium sulfate fostering alite and GGBFS dissolution at early ages. A detailed discussion about the role of the activator in hybrid binders containing GGBFS can be found a previous study of the authors (Etcheverry et al., 2023a). In this study, the inclusion of RA always reduces the compressive strength of the produced concrete, regardless of the binder type. Nevertheless, up to 3 days of hydration, the use of hybrid binder seems capable of mitigating the poorer performance as a result of the RA inclusion.

From 7 days of hydration onwards, the binder type has a lower influence on strength development and the amount of RA is the main parameter controlling the strength. Up to 90 days of hydration, the strength is reduced as RA content is increased. It appears that specifically for the concrete produced with 20% RA, a slightly higher strength

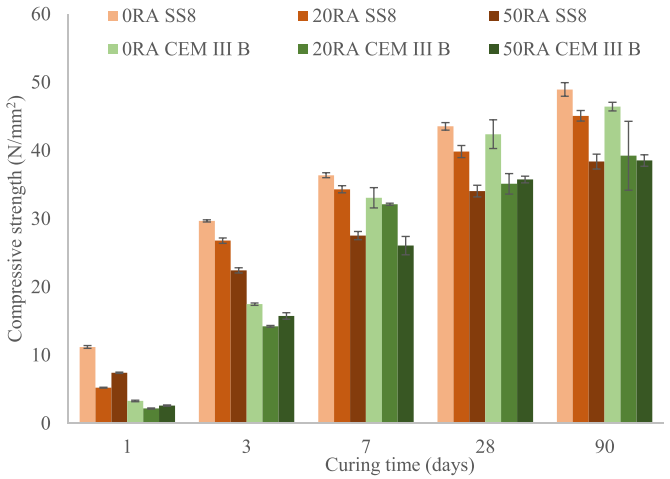

Fig. 6. Compressive strength measurements on concrete containing 0%, 20% and 50% RA for a hybrid and a commercial CEM III/B binder.

is observed at 28 and 90 days when the hybrid binder is used in comparison to the CEM III/B. A possible explanation is that concrete produced with the hybrid system remains denser than the one produced with the blended cement, thus up to a content of 20% RA, the hybrid matrix is capable of mitigating the detrimental effect of the RA.

3.4. Transport properties

The pore structure in cementitious materials is closely related to the transport properties. Thus, the connectivity of the pore structure gives account of how easily fluids and gases can ingress the concrete. Even though porosity is an intrinsic characteristic of the cementitious matrix, understanding the pore structure (and its connectivity) in concrete is much more complex as other variables come into play. Among them, the inclusion of aggregates of different sizes and shapes generates voids that remain in the mixture. The way the concrete is compacted, the consistency, the different interfacial transition zones, the presence of RA with a greater porosity than that of natural aggregates and the way in which the greater absorption of these aggregates is compensated in the mix design, are parameters that induce changes in the pore structure. In addition, the inclusion of supplementary cementitious materials and the water-cement ratio have a great influence. All these variables, varying simultaneously, make it extremely difficult to explain the changes generated in the pore structure.

Three techniques were used to assess the pore structure: (1) density and water absorption, (2) capillary imbibition, and (3) Torrent permeability.

Fig. 7 shows the density of the concrete with and without RA. A reduction in density is observed with the increase in the RA content (Villagran et al., 2022). This is in agreement with the lower density of the RA in comparison to the NA. Concrete produced with the hybrid binder shows densities slightly higher than the ones observed for the CEM III/B system, corresponding to a greater formation of reaction products at a given hydration time as reported by (Etcheverry et al., 2023a).

It is important to note that the density decreases relatively proportional to the content of RA, while the increase in the water absorption (WA) is limited from 0%RA to 20%RA compared to the further increase from 20%RA to 50%RA (i.e., it is not linear). RA are porous particles embedded in the new cementitious matrix. It appears that the content of 20%RA remains too low to cause significant effect on the total porosity (obtained from vacuum saturation of samples).

The embedment of this low content of RA seems to reduce the impact of the RA below the impact it would be expected considering the relative volume of the RA replacement. This observation is opposite to what is observed later for capillary absorption and carbonation due to the fact that WA measures the total volume of pores because samples are vacuum saturated. For the other properties, parameters such as the pore size distribution and connectivity are more relevant. Meaning that a grater absorption of water and a lower density do not necessarily entail a worse performance in terms of durability.

Fig. 8 shows the results of the capillary imbibition test. These curves are the average values from 3 samples. It can be observed that both binders behave similarly in terms of water gain.

The addition of RA seems to have the biggest influence on the results regardless of the binder type. An increased water gain is observed for mixes containing RA since the first measured value. However, increasing the amount of RA in the concrete appears to have a limited effect on the water gain supporting the idea that RA embedment in a dense cementitious matrix reduce the impact of the RA despite the higher WA and lower density discussed in the previous section. These observations are in agreement with the CIC (Table 4), which increases with the RA aggregate addition, but moving from 20% RA to 50% RA does not seems to have such a big influence as moving from 0 to 20%, highlighting predominant the impact of the connectivity and pore distribution of the new cementitious matrix enclosing the RA.

When it comes to Torrent measurements, all concrete mixes, regardless of RA content or binder type (hybrid versus blended), exhibited a KT (10^{-16} m^2) value below 0.1 (refer to Table S3 in the supporting information file). Therefore, all the concrete mixes in this study meet the stringent requirements outlined in SIA 262 for structures exposed to chlorides, where a KT value below 0.5 is required. Results of

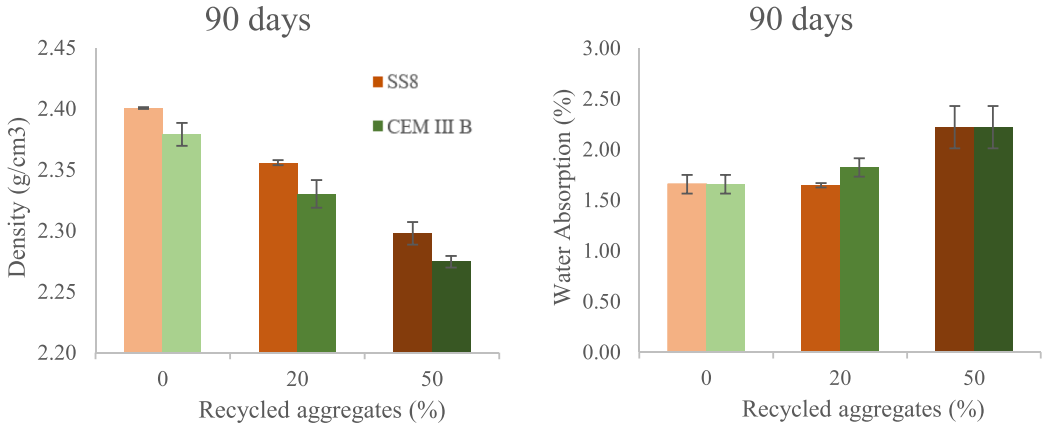

Fig. 7. Density and water absorption (40 °C) of concrete containing variable replacement of natural aggregate by RA.

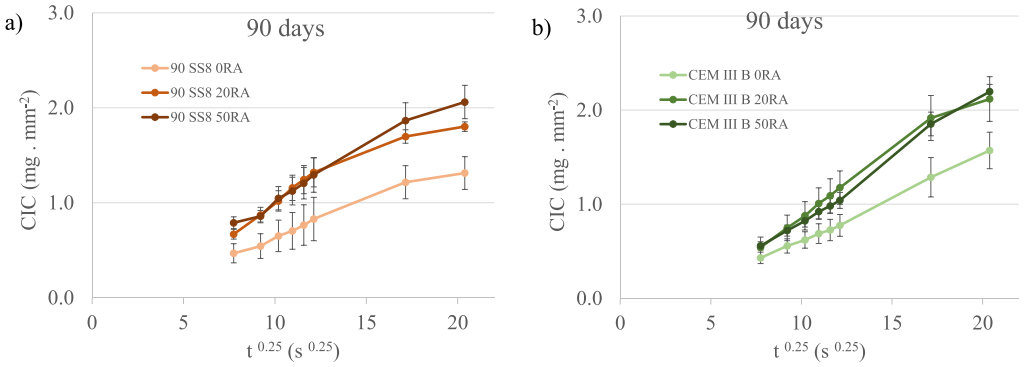

Fig. 8. Results of capillary imbibition test during the first 48 h for a hybrid cement after 90 days of curing (a) and a commercial CEM III/B after 90 days of curing (b).

Table 4
Capillary imbibition coefficient (mg/mm^2) for the 6 concrete types after 90 days of hydration. CIC calculated considering the first 24 h of absorption.

	SS8		CEM III/B	
	CIC	R^2	CIC	R^2
0% RA	0.071	0.999	0.062	0.998
20% RA	0.103	0.995	0.096	0.984
50% RA	0.122	0.999	0.097	0.983

water penetration under pressure showed a limited penetration depth and difference among concrete mixes (Fig. S2).

3.5. Durability

3.5.1. Chloride resistance and electrical resistivity

Fig. 9 plots the results of the rapid chloride migration test for concrete with hybrid and blended binder with variable contents of RA. In this case, a very limited influence of the curing time (28 days versus 90 days) is observed for any of the mixes. A statistical test (multiple comparison of means by Student-Newman-Keuls test at significance level of 0.05 using IBM SPSS Statistics 29.0) revealed that the amount of RA does not have a significant influence. The effective levels of significance obtained were: 0.065 for the series CEM III/B with 0, 20 and 50% RA and 0.205 for SS8 with 0, 20 and 50% RA. Therefore, it is concluded that the migration coefficients remain in the same range when in concrete mixes with the same binder type the RA content is varied, with average values for the non-steady state migration coefficient of 3.8–5 $\times$ 10^{-12} m^2/s for SS8 or from 7.2 to 6.5 $\times$ 10^{-12} m^2/s for CEM III/B. The higher porosity and shortcut effect provided by the addition of the RA may be (completely or partially) compensated by the higher amount of paste in the systems as explained by (Villagran et al., 2022). The main difference was observed between binder types with the hybrid binder showing lower non-steady-state migration coefficients than mixes with CEM III/B.

It is important to note that all concrete mixes tested in this study are within the limits of the most demanding category for durability in terms of chloride environments (chloride migration coefficient (10^{-12} m^2/s) D < 10) defined by the Swiss Standard (SIA 262). Measurements of bulk resistivity (Fig. 10) are normally used as an indicator for the quality of the concrete cover. The resistivity of concrete can be classified in four categories: <100; 100–500; 500–1000 and > 1000 Ω m (Metals et al., 1997), where the risk of corrosion decreases as the resistivity increases, resulting in the following classification: high, moderate, low and negligible risk of corrosion. Results shown in Fig. 8 support the good performance measured by the rapid CMT and all concretes in this study falls in the negligible risk range. Concrete mixes containing GGBFS thrive in these environments because of the ability of the aluminium-rich phases to bind chlorides (Loser et al., 2010), (Shi et al., 2017). The phase assemblage of a commercial binder (CEM III/B) versus a hybrid one was further discussed in one of our previous works (Etcheverry et al., 2023b), where a greater amount of Al in C-(A-)S–H, ettringite and AFm phases were observed for the hybrid system at a given age. This greater amount of C-A-S-H and AFm phases appears to be

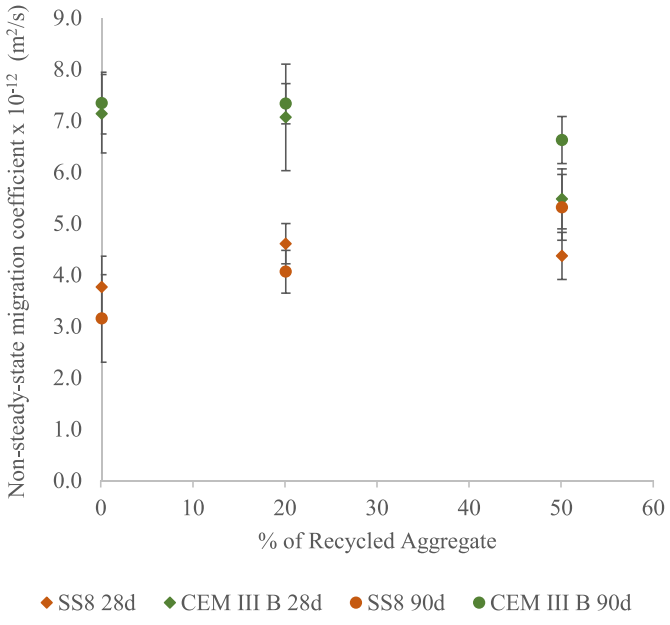

Fig. 9. Results of the rapid chloride migration test in concretes containing 0, 20 and 50% RA and two binder types.

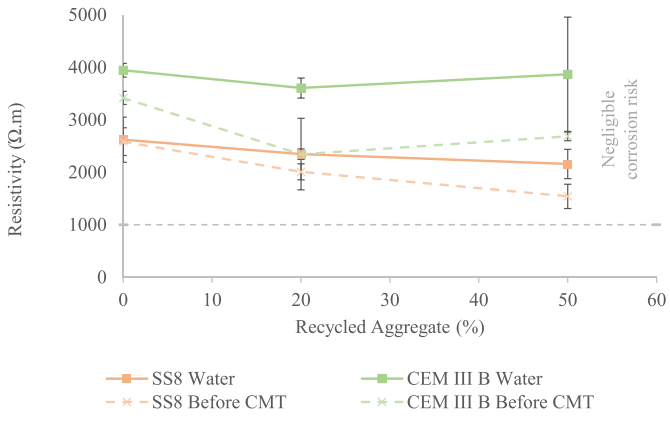

Fig. 10. Values of resistivity for samples (90 days) impregnated with water and with the calcium chloride solution before the beginning of the rapid CMT.

the reason behind the better CMT results for the hybrid binder. However, the lower D-values for the hybrid binder shown in Fig. 9 can also be associated to a denser microstructure. Detail information about the voltage potential under which the samples were tested is included in Table S2 (supporting information file).

At similar level of alkalis, a higher resistivity is associated with a denser microstructure (Bu and Weiss, 2014). Results of bulk resistivity measured before CMT (or in water impregnated samples), seem to reveal that there is a minor decrease in the resistivity of the samples when RA have been included. Nevertheless, the fact that the old cementitious matrix present in the RA can contribute to chloride binding, appears to compensate for the greater porosity and pore connectivity in the RA samples, leading to similar migration coefficients.

The higher resistivity observed for the hybrid binder in comparison to CEM III/B mixes (Fig. 10) should not be interpreted as a worse performance. The pore solution resistivity is strongly influence by the alkali content of the binder. Alkali species such as sodium or hydroxide ions make the pore solution more conductive, thus lower the resistivity (Snyder et al., 2003).

3.5.2. Carbonation performance

The results of the carbonation test for the (a) hybrid system and the (b) commercial CEM III/B system with variable contents of RA are shown in Fig. 11. The addition of RA increases the carbonation rate, resulting in a concrete more prone to carbonation in all cases. This effect is more pronounced for the hybrid binder where the addition of 50%RA results in a carbonation front twice as deep as for the reference without RA after one year of exposure. A more limited difference (but an overall worse performance) is observed with the RA replacement for the CEM III/B mixes.

A better performance observed for the hybrid binder over the commercial CEM III/B is related to a denser microstructure, which seems not only in agreement with the results presented in Fig. 8, but also with previous studies (Etcheverry et al., 2023a), (Fu et al., 2020). This statement is reinforced by the computation of the w/CaO ratios or (since all mixes have the same w/b ratio) the CaO content (Escalante-Garcia et al., 2021), (Gluth et al., 2022). Both binders present a similar amount of CaO (45.3% for SS8 and 46.6% for CEM III/B) which suggests a similar CO_2 binding capacity, thus, the difference must be linked to either microstructure development (as mentioned above based on previous observations) or to possible differences in the pore solution delaying the carbonation in the hybrid system. For instance, carbonation in presence of a higher alkalis content would lead to the precipitation of vaterite as an intermediate product instead of calcite, and smaller calcite crystal sizes were observed at low content of alkalis (Zajac et al., 2021). In addition, alkalis in a high amount seems to prevent the precipitation of gypsum after carbonation. This is relevant cause the precipitation of gypsum can reduce the carbon capture capacity of the binder due to the fact that less calcium is present to form $CaCO_3$ (Zajac et al., 2022).

The substitution of natural aggregate by more porous RA seems to act as a shortcut for the CO_2 to go through the denser paste (in the hybrid binder than in CEM III/B). Therefore, the effect of the dense paste is reduced as the percentage of RA increases. Under accelerated conditions (Fig. S3 supporting information file) a similar trend is observed, i.e., the shortcut created by the addition of RA affects the carbonation performance but the hybrid binder still performs better than CEM III/B mixes. Establishing a correlation between natural and accelerated carbonation rate is out of the scope of this paper, and accelerated experiments (Fig. S3 in the supporting information file) were included to support the explanation about the shortcut created by RA.

A hypothesis to explain the varying effects of RA depending on the binder type considers the role of moisture equilibrium achieved with the exposure atmosphere. The particular pore solution chemistry for each binder may result in different saturation degrees under a 65% RH environment. This means that even though they were exposed in the same environment, concrete with the hybrid binder and CEM III/B may have achieved different saturation degrees at equilibrium. This is based on the fact that, when exposed to the same environment, alkali-activated binders have been reported to achieve a higher saturation degree compared to Portland cement paste (Babaee and Castel, 2018). The hybrid binder examined in the present study falls between these two cases, yet it is closer to alkali-activated binders than CEM III/B used here as reference. The inclusion of sodium ions in the pore solution, due to the use of the activator in the hybrid system, promotes the retention of evaporable water at a given RH on the moisture isotherm (Materials, 1987). This higher saturation degree likely reduces the transport of CO_2 across a broader pore size range that remains saturated in the hybrid system compared to the CEM III/B system. Additionally, the attached cement paste that makes part of RA particles has a pore chemistry more akin to the CEM III/B matrix than to the hybrid binder matrix. Therefore, the saturation degree of the concrete may vary more with the RA content when in combination with the hybrid binder than with CEM III/B. This hypothesis requires further research to understand the effects of the pore chemistry of hybrid binders on moisture isotherms and the

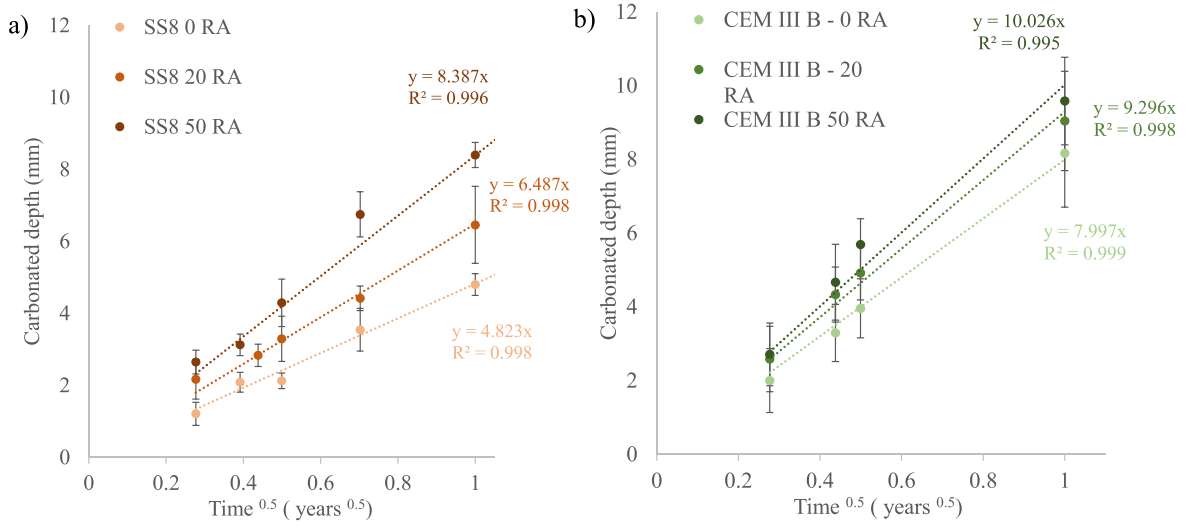

Fig. 11. Carbonation depth measured in concrete with a variable amount of RA. (a) hybrid binder and (b) commercial CEM III/B under natural exposure conditions (indoor).

resulting transport properties of the matrix. This includes additional studies to determine how the carbonation performance is influenced by the equilibrium concrete pore solution.

3.6. Environmental impact assessment

This section introduces the results of the impact assessment, particularly referring to CO_2 emissions in two parts, namely manufacturing stage (cradle-to-gate) and cradle-to-use.

3.6.1. Manufacturing stage

The total CO_2 emissions (in kg) associated to the manufacturing of 1 m^3 of concrete and the percentual contribution of each component to the indicator is show in Fig. 12. An important remark is that the impact of the transportation of each component is part of its own impact.

To begin with, it is observed (Fig. 12) that the production of the binder in all cases contributes to around 75% of the total CO_2 emissions, followed by around 15% for the production of the aggregates (natural and recycled), 10% for sand production and a negligible impact is attributed to the alkali activator (<2%). Furthermore, the concrete mixes SS8 have a slightly higher environmental impact (3–4%) in comparison to the mixes with CEM III/B. A probable reason behind is that the CEM III/B production was modelled by a generic dataset which might apply a small difference in the allocation attributed to the GGBFS compared to the one in the SS8 series (Etcheverry et al., 2023a). It is also interesting to mention that the replacement of natural aggregate by RA does not help to significantly reduce the CO_2 emissions, since their production brings similar impacts in terms of CO_2 emissions associated to production and transport, but it can indirectly contribute to it by the avoided effect of the landfilling (with transportation distances playing a significant role) (Villagran et al., 2023). The transportation of the C&DW (100 km) and the required intermediate treatments in which electricity is consumed (35% provided by fossil fuels) explain this result. The optimization of the transportation distance and a switch to more eco-efficient energy mixes can play a decisive role, also considering that aggregates represent the largest share in the mix (see Table 2). Although from a CO_2 reduction point of view, the use of RA is not as effective as changing the binder type, the use of RA in combination with hybrid binders seems promising. In addition, the pre-carbonation of RA holds promise to reduce the initial footprint of the RA (Zhang et al., 2015), (Kaddah et al., 2022), while contributing to balance concrete properties and other impact indicators, like the consumption of natural raw materials (resource efficiency).

In general, considering the cradle-to-gate stages, both circular economy strategies do not seem to provide significant reductions to the CO2–C indicator. However, this analysis is made per volume of produced concrete, without considering the mechanical and durability properties of each concrete mix, therefore giving an unfair comparison.

3.6.2. Cradle-to-use: integration of manufacturing emissions, mechanical and durability properties

This section is dedicated to integrating the CO_2 emissions at manufacturing stage of the concrete mixes with their mechanical and durability performance during the use phase. First, the ratio of CO_2 emissions per m^3 and MPa (Eq. (1)) for each CES concrete related to the reference is shown in Fig. 13. Fig. 14 summarises the results of the combined effect of compressive strength, chloride diffusion and carbonation (Equations (2)–(4)), expressed as the ratio between the CES and the reference. In both figures, the red dotted line at the value 1,

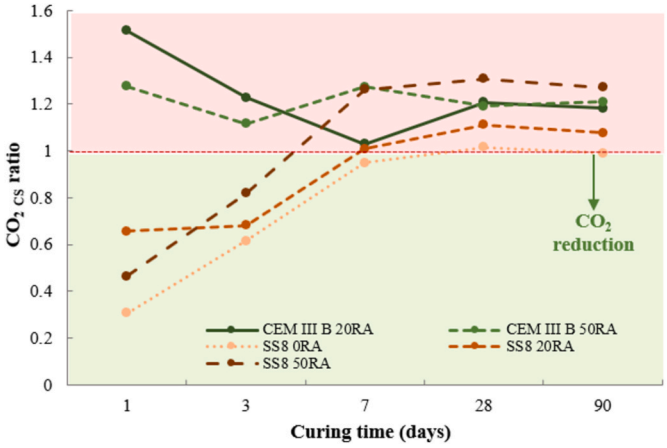

Fig. 13. Ratio of CO_2 emissions per m^3 and MPa for each CES concrete related to the reference (CEM III/B 0RA).

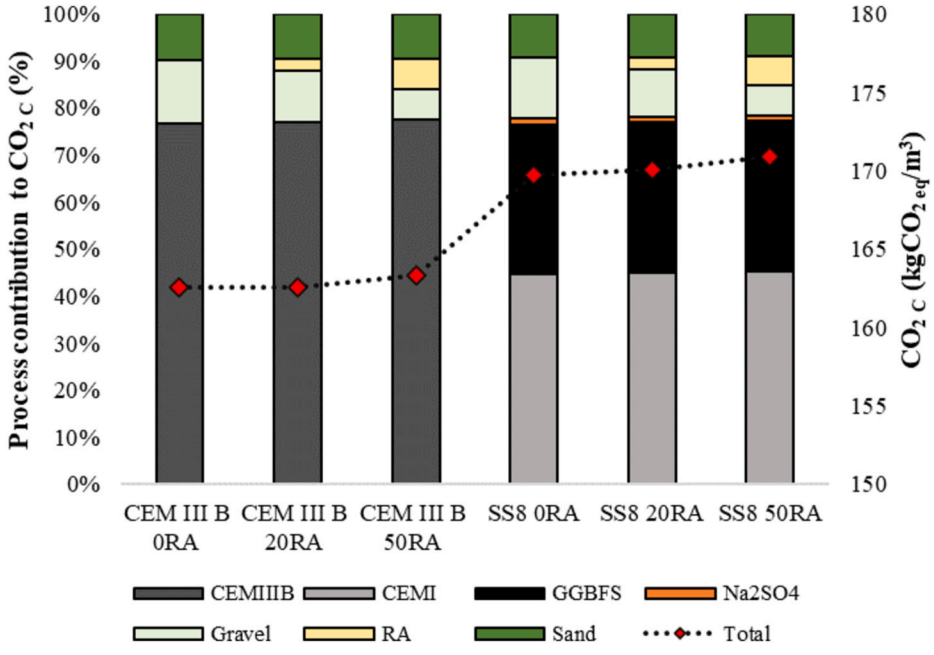

Fig. 12. Total cradle-to-gate CO_2 emissions per m^3 of concrete and process contribution.

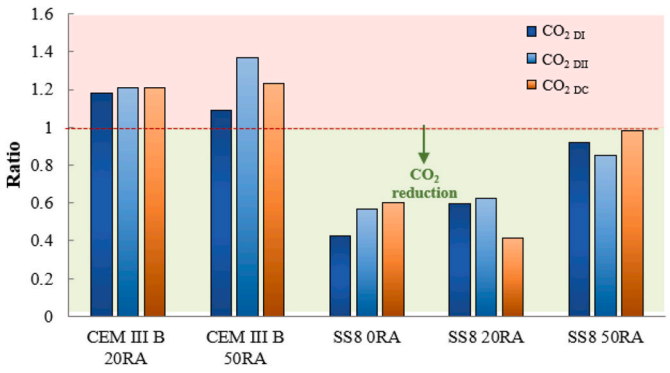

Fig. 14. CO_2-DI, CO_2-DII and CO_2-DC ratios comparing the CES concrete emissions to the reference.

indicates the CO_2 reduction zone. All samples located in the green zone, lead to a reduction in the total CO_2 emissions while keeping comparable or better performance than the reference concrete.

In Fig. 13 it can be observed that although the initial emissions per m^3 are fixed (Section 3.6.1), the CO_2-CS indicator evolves differently according to the curing age. As was observed before, at early age (1–3 days) the series SS8 have a significantly better performance than the concrete mix with commercial CEM III/B. At 1 day reductions of the CO_2-CS indicator between 30 and 70% with respect to the reference can be obtained, depending on the content of RA. At 3 days the reductions are attenuated (20–40%) because the GGBFS in the CEM III/B reference starts to react and thus contributes to the development of the strength, which reduces the strength difference with the SS8 binder systems (Section 3.3). Although not here quantified, from a constructive perspective these results can have positive impacts. Higher early strength means lower sensitivity of the concrete to adverse curing conditions such as low humidity or low temperatures and capability to early removal of formworks with less risks, among others. From 7 days on, only the sample SS8 0RA manages to have similar CO_2 emissions while maintaining comparable strength as the CEM III/B reference. In this Figure it is also noted that the circular economy strategy using RA alone does not lead to reductions of CO_2 at any curing age, as the values are above 1. It is also highlighted that an increase of the RA proportion at later ages in all concrete types leads to an increment in CO_2 emissions/MPa. A pre-carbonation treatment of the RA could lead to generate an aggregate with better properties (thus positive impact in concrete) while contributing at the same time to CO2 sequestration.

In general, especially at early ages, the SS8 series entails lower CO_2 emissions per MPa than a commercial CEM III/B with similar amount of RA. This demonstrates that the combined circular economy strategy of using RA in combination with a hybrid alkali activated GGBFS binder is more efficient than the use of RA alone. Finally, a remarkable lesson from Fig. 13 in terms of decision making is that when considering mechanical performance and cradle-to-gate emissions to compare between different concretes, the curing age has a significant influence and it can lead to incorrect decisions if not applied properly considering the requirements in the field.

The combined effect of compressive strength and durability parameters is shown in Fig. 13. It should be noted that the compressive strength, the chloride diffusion, and carbonation coefficients are taken at the same curing age of 90 days. As can be observed in Fig. 13, all samples at 90 days are located near or above the red dotted line. This means that any reduction or increment in the CO_2 emissions compared to the reference in Fig. 14 are purely because of a better or worse durability performance.

The results shown in Fig. 14 clearly depend on the type of durability parameter considered. A significant reduction in the chloride migration coefficient was obtained when the hybrid binder is used instead of commercial CEM III/B (Fig. 6). This fact is reflected in the CO_2-DI coefficient, which in all cases is below 1 for the SS8 series, indicating the positive effect of the hybrid binder to reduce the CO_2 emissions while meeting the mechanical and durability requirements. The use of RA negatively affects mostly the concrete with commercial cement, which show an increase of the indicator values. For the SS8 series it can be clearly seen that the use of 20% RA has no negative effects, while 50% of RA minimizes the benefits with respect to the reference. A similar conclusion can be drawn when considering the carbonation coefficient in the indicator CO_2-DII. The potential denser microstructure generated by the hybrid binder (compared to commercial CEM III/B) leads to a lower carbonation coefficient than the reference. It is relevant mention that here carbonation is seen as a deterioration phenomenon that can lead to lower durability. However, in non-reinforced concrete where corrosion is not a problem, the CO2 uptake could be beneficial.

All hybrid-binder concretes of series SS8 are located in the CO_2 reduction zone of Fig. 13, corroborating once more the superior performance of the combined circular economy strategy in the design of the concretes for reinforced concrete applications. When the durability against carbonation and chlorides both need to be considered along with mechanical performance, the CO_2-DC indicator reveals the same trend as previously observed for the chloride diffusion and carbonation coefficient separately. If an integral performance is considered, the sample SS8 20RA shows the lowest CO2-DC ratio. All in all, the SS8 series have consistently shown their potential to reduce CO_2 emissions compared to a reference concrete mix with natural aggregate and commercial CEM III/B, while meeting the mechanical and durability requirements. This solution conciliates the simultaneous transition towards a low carbon and circular concrete industry for efficient use of resources while producing good quality concretes.

4. Conclusions

This study discusses various aspects of concrete produced with recycled aggregates from C&DW and two binder types, a CEM III/B and a hybrid binder with 70% GGBFS and 30% PC activated by sodium sulfate, and the main outcomes are.

1. Increased recycled aggregates content leads to lower density and a higher porosity of the concrete in comparison to the reference mix with natural aggregates. The hybrid binder effectively increased the early age strength, and the influence of the activator surpasses the negative effect caused by the inclusion of low-quality RA.
2. In terms of transport properties and durability, there is a combined effect of the binder and recycled aggregate content. However, the influence of the aggregate replacement is highly dependent on the recycled aggregate quality. In this study, all concrete types meet high-quality standards for chloride resistance with bulk resistivity measurements indicating a negligible risk of corrosion. In terms of carbonation performance, the RAs increased carbonation rate.
3. The main contribution in terms of CO_2 emission comes from the binder production. Concrete mixes prepared with the hybrid system show comparable cradle-to-gate CO_2 emissions per cubic meter of concrete. Nevertheless, mechanical properties and durability still need to be considered. The recycled aggregates have a comparable impact to natural aggregates in terms of CO_2 emissions but their use helps to reduce the consumption of raw materials.
4. When the early mechanical performance (compressive strength at $<$ 3 days) of the binder is considered in the calculations, the hybrid binder (with any percentage of recycled aggregates) is preferred in terms of CO_2 emissions per MPa. If only compressive strength requirements at 28 days are considered, the mixes with the two binder types are equivalent.
5. When the performance during service life (compressive strength + durability) is considered, the hybrid binder shows clear advantages. The inclusion of C&DW recycled aggregates in concrete with commercial cement (CEM III/B) results in a poorer environmental

performance than the reference with natural aggregates. Instead, hybrid mixes containing up to 20% recycled aggregates significantly improved the environmental performance and 50% replacement showed comparative results to the reference mix (CEM III/B 0% RA).

This study shows that the approach towards low carbon and circular concrete production can be balanced to comply both objectives. In the process, the requirements in the field as well as durability parameters need to be considered to successfully achieve more sustainable concrete mixes.

CRediT authorship contribution statement

Juan Manuel Etcheverry: Writing – review & editing, Writing – original draft, Visualization, Methodology, Formal analysis, Data curation, Conceptualization. **Agustin Laveglia:** Writing – review & editing, Visualization, Methodology, Investigation, Formal analysis, Conceptualization. **Yury Andres Villagran-Zaccardi:** Writing – review & editing, Visualization, Supervision, Methodology, Investigation, Conceptualization. **Nele De Belie:** Writing – review & editing, Supervision, Resources, Project administration, Methodology, Funding acquisition.

Declaration of competing interest

The authors declare that they have no known competing financial interests or personal relationships that could have appeared to influence the work reported in this paper.

Data availability

Data will be made available on request.

Acknowledgements

This research was funded by the Research Foundation-Flanders (FWO-Vlaanderen) through research grants G062720N (J.M. Etcheverry), MSCA-SoE 12ZZD21N LV (YA. Villagrán-Zaccardi), and H2020 MSCA SUBLime (A. Laveglia). This Project has received funding from the European Union's Horizon 2020 research and innovation programme under Marie Sklodowska-Curie project SUBLime [Grant Agreement n°955986].

Appendix A. Supplementary data

Supplementary data to this article can be found online at https://doi.org/10.1016/j.dibe.2024.100370.

References

Abbas, A., Fathifazl, G., Isgor, O.B., Razaqpur, A.G., Fournier, B., Foo, S., 2009. Cement & concrete composites durability of recycled aggregate concrete designed with equivalent mortar volume method. Cem. Concr. Compos. 31 (8), 555–563. https://doi.org/10.1016/j.cemconcomp.2009.02.012.

Acevedo-Martinez, E., Gomez-Zamorano, L.Y., Escalante-Garcia, J.I., 2012. Portland cement-blast furnace slag mortars activated using waterglass: - Part 1: effect of slag replacement and alkali concentration. Construct. Build. Mater. 37, 462–469. https://doi.org/10.1016/j.conbuildmat.2012.07.041.

Babaee, M., Castel, A., 2018. Cement and Concrete Research Water vapor sorption isotherms , pore structure , and moisture transport characteristics of alkali-activated and Portland cement-based binders. Cement Concr. Res. 113, 99–120. https://doi.org/10.1016/j.cemconres.2018.07.006. July.

Bernal, S.A., 2016. Advances in near-neutral salts activation of blast furnace slags. RILEM Tech. Lett. 1, 39. https://doi.org/10.21809/rilemtechlett.v1.8.

Bu, Y., Weiss, J., 2014. Cement & Concrete Composites the influence of alkali content on the electrical resistivity and transport properties of cementitious materials. Cem. Concr. Compos. 51, 49–58. https://doi.org/10.1016/j.cemconcomp.2014.02.008.

Di Maio, A.A., 2010. Effect of Natural Coarse Aggregate Type on the Physical and Mechanical Properties of Recycled Coarse Aggregates, pp. 195–202. https://doi.org/10.1617/s11527-009-9480-4.

Etcheverry, J.M., Villagran-zaccardi, Y.A., Van den Heede, P., Hallet, V., De Belie, N., 2023a. Effect of sodium sulfate activation on the early age behaviour and microstructure development of hybrid cementitious systems containing Portland cement and blast furnace slag. Cem. Concr. Compos. 141 (December 2022), 105101 https://doi.org/10.1016/j.cemconcomp.2023.105101.

Etcheverry, J.M., et al., 2023b. Phase evolution of hybrid alkali sulfate-activated ground-granulated blast furnace slag cements. ACS Sustain. Chem. Eng. https://doi.org/10.1021/acssuschemeng.3c05937.

European Environment Agency, E.R., 2008. Effectiveness of environmental taxes and charges for managing sand, gravel and rock extraction in selected EU countries, 2.

Fu, J., et al., 2020. Mechanisms of enhancement in early hydration by sodium sulfate in a slag-cement blend – Insights from pore solution chemistry. Cement Concr. Res. 135 https://doi.org/10.1016/j.cemconres.2020.106110. November 2019.

Fu, J., et al., 2021a. A microstructural investigation of a Na2SO4 activated cement-slag blend. Cement Concr. Res. 150, 106609 https://doi.org/10.1016/j.cemconres.2021.106609. December 2020.

Fu, J., et al., 2021b. Cement and Concrete Research A microstructural investigation of a Na 2 SO 4 activated cement-slag blend. Cement Concr. Res. 150 (September), 106609 https://doi.org/10.1016/j.cemconres.2021.106609.

Gluth, G.J.G., et al., 2022. Carbonation rate of alkali-activated concretes and high-volume SCM concretes : a literature data analysis by RILEM TC 281-CCC. Mater. Struct. 4 https://doi.org/10.1617/s11527-022-02041-4.

Joa, B.L., 2013. Workability Study of Concretes Made with Recycled Mortar Aggregate, pp. 1765–1778. https://doi.org/10.1617/s11527-012-0010-4.

Jolliet, O., Margni, M., Charles, R., Humbert, S., Payet, J., Rebitzer, G., 2003. Presemmg a new Meth6d IMPACT 2002 + : a new life cycle impact assessment methodology, 8 (6), 324–330.

Joseph, S., Snellings, R., Cizer, Ö., 2019. Activation of Portland cement blended with high volume of fly ash using Na2SO4. Cem. Concr. Compos. 104 (September), 103417 https://doi.org/10.1016/j.cemconcomp.2019.103417.

Kaddah, F., Ranaivomanana, H., Amiri, O., Rozi, E., 2022. Accelerated carbonation of recycled concrete aggregates : investigation on the microstructure and transport properties at cement paste and mortar scales. September 57, 1–11. https://doi.org/10.1016/j.jcou.2022.101885, 2021.

Krüger, M., Bregar, R., David, G.A., Juhart, J., 2016. Non-destructive evaluation of eco-friendly cementituous materials by ultrasound. Proc. Int. RILEM Conf. Mater. Syst. Struct. Civ. Eng. (August), 503–512.

Kurz, J.H., Grosse, C.U., Reinhardt, H.W., 2005. Strategies for reliable automatic onset time picking of acoustic emissions and of ultrasound signals in concrete. Ultrasonics 43 (7), 538–546. https://doi.org/10.1016/j.ultras.2004.12.005.

Laveglia, A., Sambataro, L., Ukrainczyk, N., De Belie, N., Koenders, E., 2022. Hydrated lime life-cycle assessment : current and future scenarios in four EU countries BE IR. J. Clean. Prod. 369, 133224 https://doi.org/10.1016/j.jclepro.2022.133224. February.

Laveglia, A., Ukrainczyk, N., De Belie, N., Koenders, E., 2023. Decarbonizing the lime-based construction materials industry : a practical guide for cradle-to-gate life-cycle inventory. Sustain. Prod. Consum. 40, 194–209. https://doi.org/10.1016/j.spc.2023.06.021. June.

Loser, R., Lothenbach, B., Leemann, A., Tuchschmid, M., 2010. Cement & Concrete Composites Chloride resistance of concrete and its binding capacity – comparison between experimental results and thermodynamic modeling. Cem. Concr. Compos. 32 (1), 34–42. https://doi.org/10.1016/j.cemconcomp.2009.08.001.

Marsh, A.T.M., Velenturf, A.P.M., Bernal, S.A., 2022. Circular Economy strategies for concrete: implementation and integration. J. Clean. Prod. 362 (May), 132486 https://doi.org/10.1016/j.jclepro.2022.132486.

Escalante-Garcia, J. Ivan, Castro Borges, Pedro, Duran-Herrera, Alejandro, 2021. Proceedings of the 75th RILEM Annual Week 2021, doi: 10.1007/978-3-031-21735-7, ISBNs978-3-03-121734-0, 978-3-03-121735-7.

Materials, B., 1987. Effect of soluble salt on the sorption isotherm. Hedenblad, G., 1987. (Report TVBM; Vol. 3035, 1-10). Division of Building Materials, LTH, Lund University.

Mcneil, K., Kang, T.H., 2013. Recycled Concrete Aggregates : A Review 7 (1), 61–69. https://doi.org/10.1007/s40069-013-0032-5.

Metals, O.F., Contact, I.N., Concrete, W., 1997. Material Science. ISBN/ISSN: 92-828-0252-3.

Mota, B., Matschei, T., Scrivener, K., 2015. The influence of sodium salts and gypsum on alite hydration. Cement Concr. Res. 75, 53–65. https://doi.org/10.1016/j.cemconres.2015.04.015.

Rashad, A.M., 2015. Influence of different additives on the properties of sodium sulfate activated slag. Construct. Build. Mater. 79, 379–389. https://doi.org/10.1016/j.conbuildmat.2015.01.022.

Rashad, A.M., Bai, Y., Basheer, P.A.M., Collier, N.C., Milestone, N.B., 2012. Cement and Concrete Research Chemical and mechanical stability of sodium sulfate activated slag after exposure to elevated temperature. Cement Concr. Res. 42 (2), 333–343. https://doi.org/10.1016/j.cemconres.2011.10.007.

Rashad, A.M., Bai, Y., Basheer, P.A.M., Milestone, N.B., Collier, N.C., 2013. Hydration and properties of sodium sulfate activated slag. Cem. Concr. Compos. 37 (1), 20–29. https://doi.org/10.1016/j.cemconcomp.2012.12.010.

Reinhardt, H.W., Grosse, C.U., 2004. Continuous monitoring of setting and hardening of mortar and concrete. Construct. Build. Mater. 18 (3), 145–154. https://doi.org/10.1016/j.conbuildmat.2003.10.002.

Scrivener, K.L., John, V.M., Gartner, E.M., 2018. Eco-efficient cements: potential economically viable solutions for a low-CO2 cement-based materials industry. Cement Concr. Res. 114, 2–26. https://doi.org/10.1016/j.cemconres.2018.03.015. June.

Shi, Z., et al., 2017. Friedel's salt profiles from thermogravimetric analysis and thermodynamic modelling of Portland cement-based mortars exposed to sodium chloride solution, 78. https://doi.org/10.1016/j.cemconcomp.2017.01.002.

Smartmote - Universität Stuttgart, 2012. "FreshCon Duo User Manual," No. V.4.00 September 2012, 0–34 [Online]. Available: http://www.smartmote.de.

Snyder, K.A., Feng, X., Keen, B.D., Mason, T.O., 2003. Estimating the electrical conductivity of cement paste pore solutions from OH À. K + and Na + concentrations 33, 793–798. https://doi.org/10.1016/S0008-8846(02)01068-2.

Trtnik, G., Gams, M., 2013. The use of frequency spectrum of ultrasonic P-waves to monitor the setting process of cement pastes. Cement Concr. Res. 43 (1), 1–11. https://doi.org/10.1016/j.cemconres.2012.10.002.

Villagrán-Zaccardi, Y.A., Pico-Cortés, C.M., Etcheverry, J.M., Santillán, L.R., Sosa, M.E., 2022. Insights on the corrosion resistance of reinforced recycled aggregate concrete. Corros. Mater. Degrad. 3 (2), 192–209. https://doi.org/10.3390/cmd3020011.

Villagran, Y.A., Pico-Cortez, C.M., Etcheverry, J.M., Santillan, L.R., Sosa, E., 2022. Insights on the Corrosion Resistance of Reinforced Recycled Aggregate Concrete, pp. 192–209. https://doi.org/10.3390/cmd3020011.

Villagran, Y., Broodcoorens, L., Van Den Heede, P., 2023. Fine recycled concrete aggregates treated by means of wastewater and carbonation pretreatment, 1–11. https://doi.org/10.3390/su15086386.

Xue, L., Zhang, Z., Wang, H., 2021. Hydration mechanisms and durability of hybrid alkaline cements (HACs): a review. Construct. Build. Mater. 266, 121039 https://doi.org/10.1016/j.conbuildmat.2020.121039.

Zajac, M., Skibsted, J., Durdzinski, P., Ben Haha, M., 2021. Effect of alkalis on products of enforced carbonation of cement paste. Construct. Build. Mater. 291, 123203 https://doi.org/10.1016/j.conbuildmat.2021.123203.

Zajac, M., Skibsted, J., Lothenbach, B., Bullerjahn, F., Skocek, J., Ben Haha, M., 2022. Effect of sulfate on CO2 binding efficiency of recycled alkaline materials. Cement Concr. Res. 157 https://doi.org/10.1016/j.cemconres.2022.106804.

Zhang, J., Shi, C., Li, Y., Pan, X., Poon, C., Xie, Z., 2015. Influence of carbonated recycled concrete aggregate on properties of cement mortar. Construct. Build. Mater. 98, 1–7. https://doi.org/10.1016/j.conbuildmat.2015.08.087.